Critical Temperature and LE/G Phase Transitions in Monolayer Films of the Amphiphilic TEMPO Derivatives at the Air/Water Interface†

Michael J. Johnson,‡ Chinmay Majmudar,‡ Janusz J. Skolimowski,§ and Marcin Majda*,‡

Department of Chemistry, University of California at Berkeley, Berkeley, California 94720-1460, and Department of Organic Chemistry, University of Lódz, Narutowicza 68 90-136 Lódz, Poland

Received: June 18, 2001

Phase behavior of five members of a homologous series of 4-alkaneamido-2,2,6,6-tetramethyl-1-piperidinyloxy (C_nTEMPO with $n = 14$, 16, 18, 20, 22) was investigated with classical Langmuir monolayer techniques and with Brewster angle microscopy and 2D voltammetry. Surface potential data, BAM images, and 2D voltammetry showed that only C_{20}- and C_{22}TEMPO monolayers have a 2D LE/G critical point above room temperature and that the remaining three compounds with shorter alkane chains form supercritical monolayers. The unusually low values of the critical temperature for these amphiphiles was explained in terms of the molecular structure of their headgroup featuring two polar groups (the nitroxy and the amide moieties) located in the opposite positions of a bulky piperidine ring. The presence of the two polar groups causes a change of orientation of the headgroup during monolayer expansion and results in a substantial increase (ca. 50−100 Å^2/molecule) of the cross sectional area of these amphiphiles. As a result, in the expanded monolayers, the van der Waals attraction between the alkane chains is weakened as they can only partially align. The decreased cohesion within the monolayers leads to the observed decrease of their 2D critical temperature. Analysis of the plots of BAM reflected light intensity as a function of amphiphile's surface concentration obtained at different temperatures yielded the C_{20}TEMPO critical temperature of 28 °C. BAM and 2D voltammetry can both be used to precisely determine the position of the C_{22}TEMPO LE/G phase transition (98.5 Å^2/molecule at 23.5 °C). The proximity of the C_{20}TEMPO critical point to the room-temperature results in a less precise value of this phase transition (127−130 Å^2/molecule at 23.5 °C). A remarkably consistent ability of fresh line microelectrodes used in 2D voltammetry to nucleate the 2D gas phase makes this method less ambiguous and thus superior to BAM in determining the position of the LE/G phase transitions.

Introduction

The relationship between structure and properties of Langmuir monolayer films has been a subject of paramount importance in essentially all investigations of these two-dimensional molecular systems. Recent rapid progress[1] in the characterization of the condensed phase structures and phase transitions revealing rich polymorphism of the ordered phases of systems such as fatty acids can be related to new experimental techniques such as epifluorescence microscopy,[2−4] Brewster angle microscopy (BAM),[5,6] and grazing incidence X-ray diffraction.[7] While structural issues naturally dominate research concerned with ordered condensed phases, the questions addressing liquid and gaseous phases (LE, also referred to as L_1, and G) of Langmuir and the related Gibbs monolayers concern existence of the LE/G phase transition and the values of critical temperature. The relationship of the LE/G critical temperature ($T_c^{(I)}$) to the molecular structure of amphiphiles has not been systematically addressed. Precise determination of $T_c^{(I)}$ has been difficult and is known only for a few aliphatic acids and their derivatives. In the early literature, Adam and Jessop determined that at 16 °C, lauric acid, ethyl laurate, dodecyl alcohol, and myristic nitrile were above their critical point.[8,9] To date, there is no agreement in the measurements of the $T_c^{(I)}$ value for pentadecanoic acid. While several in depth investigations of this amphiphile exist in the literature, the reported values of $T_c^{(I)}$ range from 26 to 70 °C.[2,10,11] Recent ellipsometric experiments allowed Casson and Bain to determine a LE/G phase transition in Gibbs monolayers of decanol.[12] These measurements and the related results of Riegler and co-workers[13] concerning hexane and heptane monolayers on the water surface clearly indicate that the relationship of the most rudimentary elements of an amphiphile's structure and its 2D liquid−gas critical temperature should be systematically investigated as it is not well understood.

We have recently reported measurements suggesting an unusually low LE/G critical temperature of Langmuir monolayers of 4-tetradecaneamido-2,2,6,6-tetramethyl-1-piperidinyloxy (C_{14}TEMPO).[14] In this report, we address the molecular basis of this finding and present results obtained with four additional members of this homologous series with longer alkyl chains (C_{16}, C_{18}, C_{20}, and C_{22}). Our measurements involving surface pressure and surface potential measurements as well as Brewster angle microscopy (BAM) and 2D electrochemistry[15] allowed us to determine that at room temperature only C_{20}-TEMPO and C_{22}TEMPO monolayers exhibit LE/G phase transitions and that the derivatives with shorter alkyl chains are supercritical. We also expand on our earlier observation that 2D electrochemical techniques can serve to determine the position of the LE/G phase transition. To this end, we compare the capabilities of the surface pressure and surface potential measurements, Brewster angle microscopy, and 2D electro-

† Part of the special issue "Royce W. Murray Festschrift".

* Corresponding author. E-mail: majda@socrates.berkeley.edu.
‡ University of California at Berkeley.
§ University of Lódz.

10.1021/jp0122878 CCC: $20.00
Published on Web 09/13/2001

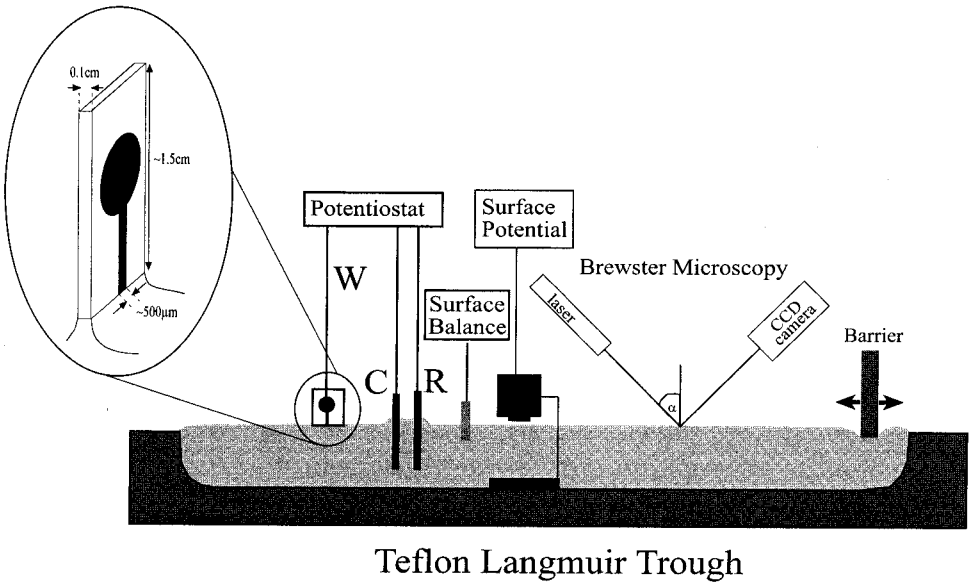

Figure 1. Schematic diagram of the experimental setup used in the characterization of the TEMPO monolayers. C, counter electrode; R, reference electrode; W, working line microelectrode. The inset shows a line microelectrode as it touches the water surface.

chemistry to determine the position of this phase transition. We find that both BAM and 2D voltammetry are quite precise. However, we show that, at least in the case of the C_{22}TEMPO monolayers, the latter technique offers a distinct advantage.

Experimental Section

Reagents. House-distilled H_2O was passed through a four-cartridge Millipore purification train and a 0.2 μm hollow-fiber final filter. The resistivity of the resulting water (DI water) was >18.3 MΩ cm. Octadecyltrichlorosilane (OTS) and 3-mercaptopropyltrimethoxysilane (MPS) were from Aldrich. OTS was vacuum-distilled into sealed glass ampules, which were opened as needed immediately prior to the individual experiments. Octadecylmercaptan (OM) (Tokyo Kasei, Tokyo, Japan) was used without further purification. Concentrated HNO_3 (Fisher, ACS Certified Plus), chloroform (Fisher, ACS certified spectranalyzed), methanol (Fisher, spectroscopic grade), and all the other reagents were used as received.

Synthesis of C_nTEMPO Amphiphiles. The synthesis of the C_{14}−C_{22}TEMPO amphiphiles involved a carbodiimide assisted coupling of 4-amino-2,2,6,6-tetramethyl-1-piperidinyloxy radical (4-aminoTEMPO) with a desired aliphatic acid. 0.011 mol of 4-aminoTEMPO and 0.01 mol of a long chain carboxylic acid were dissolved in 50 mL of methylene chloride. The solution was purged with nitrogen and stirred. After 5 min, 0.01 mol of 1-[3-(Dimethylamino)propyl]-3- ethylcarbodiimide hydrochloride coupling agent was added. The cloudy orange mixture, while stirred under nitrogen overnight, slowly converted to a clear orange solution. The resulting solution was washed twice with 50 mL saturated $NaHCO_3$ and twice with 50 mL of brine and then dried with $MgSO_4$. The organic layer was collected and yielded orange crystals upon removal of the solvent. As expected, the color of the crystals becomes less intense as the length of the alkane chain in this homologous series of compounds increases, reflecting a decrease of the weight fraction of the colored nitroxide moiety in the crystals. TLC tests indicated no other major products in these samples. Column chromatography was used for further purification. The crystals were dissolved in methylene chloride, loaded onto a neutral alumina column, and eluted with methylene chloride. A single orange band moved through the column and the main part of the band was collected. Only the leading and following edge of the product band were discarded, resulting in a high yield (~70%) of a very pure product. A UV−vis spectrum of a chloroform solution of these products features are broad band with the maximum absorbance at 470 nm. The purity, a critical component in the subsequent studies of monolayer films of these compounds at the air/water interface, was ascertained by melting point measurements, CHN analysis, and pressure−area isotherms. A plot of the melting points versus alkane chain length was linear with $r^2 = 0.991$. The individual values listed in Table 1 agreed well with the available literature. Table 1 also lists the results of CHN elemental analysis. The pressure−area (π−MMA) isotherms (discussed in more details in the next section) may be used as a sensitive, qualitative test of sample's purity. Even small amounts of impurities cause irregularities such as kinks along a sharply rising section of π−MMA curves. Following their purification, our samples did not exhibit any such irregularities.

TABLE 1: Results of CHN Analysis of the TEMPO Amphiphiles

		%C		%H		%N	
compound	mp (°C)	calcd	found	calcd	found	calcd	found
C_{14}TEMPO	49.5	72.4	72.5	11.9	11.9	7.3	7.3
C_{16}TEMPO	57.5	73.3	73.2	12.1	12.2	6.8	6.8
C_{18}TEMPO	61.0	74.1	74.1	12.2	12.3	6.4	6.4
C_{20}TEMPO	69.0	74.8	74.5	12.4	12.6	6.0	6.0
C_{22}TEMPO	74.5	75.4	75.4	12.5	12.7	5.7	5.8

Experiments on the Water Surface and Monolayer Techniques. The experimental setup combining several measurement techniques addressing a monolayer film at the air/water interface in a Langmuir trough is shown schematically in Figure 1. C_{14-22}TEMPO monolayers were spread from 1.0 mM chloroform solutions at 150 Å^2/molecule and compressed at 11 Å^2/molecule per min. To minimize mechanical vibration of the water surface, Brewster angle microscopy (BAM) was performed on a small active vibrational table (MOD-2, Halcyonics GmbH, Goettingen, Germany). These instruments were enclosed in a Plexiglas box on a large table within a thermostated, laminar flow enclosure operated under positive pressure with filtered air. While, persistent building vibrations beyond our control resulted in some BAM reflected light fluctuations shown in our

data, we believe that these vibrations did not affect the mean behavior of the monolayers presented in this report.

The Brewster angle microscope (BAM2plus, Nanofilm Technologie GmbH, Goettingen, Germany) is equipped with a 50 mW Nd:YAG laser. It was typically operated at 40% power. BAM observations involving monolayer surface concentrations near phase transitions were done in short, ca. 1−3 s exposures interspersed by ca. 15 s combining to a total observation time of ca. 3 min at each surface concentration of an amphiphile. More frequent or longer exposure times were avoided under these conditions to prevent local laser beam induced temperature increases which could offset the position of phase transitions. In other experiments, the exposure time was typically 30−90 s.

Surface potential versus mean molecular area (MMA) measurements were done with a Kelvin probe (vibrating plate method, Spot1 by KSV Instruments, Ltd., Helsinki, Finland) in a large Langmuir trough equipped with two symmetrically positioned barriers (KSV 2000). Cleanliness of the air/water interface was checked before each series of measurements and was judged to be satisfactory if the change of the surface potential was less than ±5 mV after changing the position of the barriers to sweep the entire trough area and thus to compress surface impurities into a small area occupied by the Kelvin probe. Subsequently, the barriers were returned to the initial position, the surface potential reading was zeroed again, and a monolayer to be investigated was spread on the water surface.

2D Electrochemical Measurements. Electrochemical measurements at the air/water interface required specially designed "line" microelectrodes that can be positioned exactly in the plane of the air/water interface.[16] They were produced by creating a sharp gradient of wettability along a fracture line of ~800 Å thick gold films, vapor-deposited on microscope glass slides (ca. 8 × 20 mm^2). The pattern of the deposited gold film includes two circular areas, later used as electrical contact pads, and a strip of gold (0.50 mm in width) running between them. Pretreatment of the glass substrates (Corning 2947) and their subsequent treatment with 3-mercaptopropyltrimethoxysilane (MPS) to induce adhesion of the vapor-deposited gold film were described recently.[17] Following gold vapor deposition, monolayers of octadecane mercaptan (OM) and octadecyltrichlorosilane (OTS) were formed on gold and on glass surfaces, respectively, by self-assembly to render all the surfaces of the substrate hydrophobic. By breaking such an electrode substrate in half (along a line drawn with a diamond pencil on the reverse side of the glass substrate perpendicular to the gold strip), one exposes a clean, and thus hydrophilic, edge surface of glass and gold and create two identical microelectrodes. These electrodes can then be positioned at the air/water interface by touching the water surface with the newly created edge surface, as shown in Figure 1. Thus, a line of wettability is formed along the edge of the gold microband between the hydrophilic gold cross sectional area and the hydrophobic (OM-coated) front face of the gold strip. The electrodes were always positioned at the air/water interface following monolayer spreading and solvent evaporation. Their performance at the air/water interface is typically reproducible for ~30 min. Later, contamination of the microband deteriorates the electrochemical signal and the electrode must be discarded. Cyclic voltammetry was done with an Ensman Model 852 bipotentiostat (Bloomington, IN) in a three-electrode configuration under computer control. The reference electrode (SCE) and a Pt counter electrode were immersed in the subphase in a Langmuir trough behind the barrier, where their presence did not interfere with a monolayer compression.

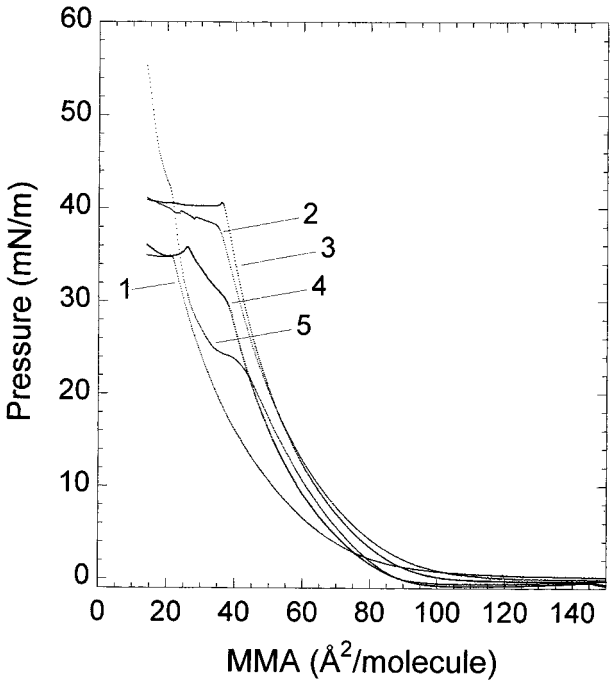

Figure 2. Set of surface pressure−MMA isotherms recorded for C_n-TEMPO amphiphiles on 50 mM HNO_3 at 23.5 °C. Curves 1−5 correspond to $n = 14-22$, respectively.

CHART 1: Chemical Structure of C_{14}TEMPO

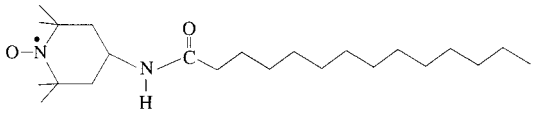

Results and Discussion

Surface Pressure and Surface Potential Isotherms. The chemical structure of C_{14}TEMPO, the shortest chain homologue of the series, is shown in Chart 1. These amphiphiles feature two polar groups in the headgroup region, the nitroxy (>N•−O) and amide groups. These are separated by a bulky, lipophilic piperidine ring with four side methyl groups. These structural features are critical to the observed phase behavior reported recently and discussed in this report.[14] Specifically, we postulate that in the high-pressure region, these compounds assume a vertical orientation of the TEMPO headgroup, minimizing their cross sectional area (see Figure 2). However, as their monolayers are expanded, the tetramethyl-1-piperidinyloxy ring tilts its N−C4 axis and ultimately assumes a roughly horizontal orientation which maximizes hydration of both of its polar fragments. In this orientation, its mean molecular area is substantially larger, 90−100 $Å^2$/molecule. As shown below, this postulate is consistent with the surface pressure observed in this region.

A set of π−MMA isotherms for all five-members of this series is shown in Figure 2. A very gradual approach of the surface pressure to $\pi = 0$ in the expansion experiments is characteristic for all these compounds. Two additional features are noteworthy. The isotherm for C_{14}TEMPO is shifted to lower mean molecular areas at higher pressures, suggesting partial solubility of this shortest chain derivative. Indeed, an increasingly larger shift was observed as a function of the decreasing compressing rate supporting this conclusion.[18] A similar shift

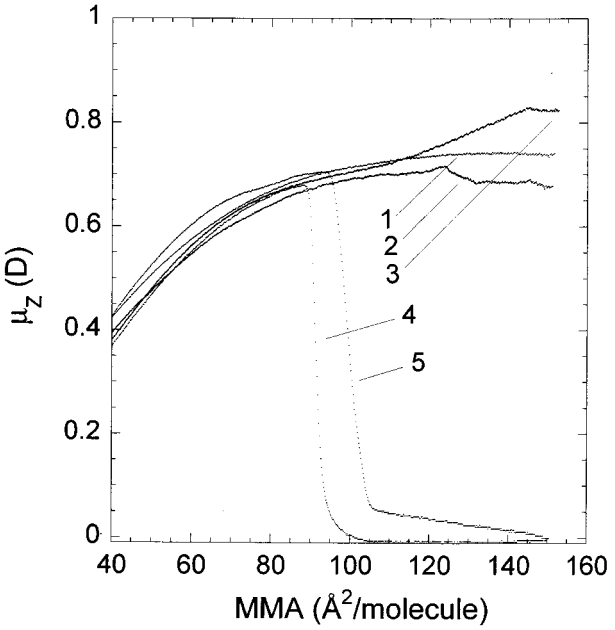

Figure 3. Set of μ_Z vs MMA data obtained from the surface potential measurements according to eq 1 on the 50 mM HNO_3 subphase at 23.5 °C. Curves 1−5 correspond to C_nTEMPO amphiphiles with $n = 14-22$, respectively.

was also observed when an increasing time was allowed to incubate the C_{14}TEMPO monolayers at a large MMA before their constant rate compression was initiated. The other observation is the inverse dependence of the collapse pressure on the chain length, which reflects the increasing rigidity of the liquid monolayers with the increasing chain length.

During monolayer expansion, the mean molecular area at which pressure assumes a value independent of further expansion (approximately $\pi = 0$) is usually associated with the onset of the liquid/gas (LE/G) phase transition.[9] Alternatively, the so-called pressure takeoff point recorded during monolayer compression is interpreted as the end of the LE-G coexistence region. Clearly, in the case of the C_nTEMPO isotherms, this method of determining the existence and the position of the LE/G phase transition is neither precise nor accurate. Specifically, the C_{20} and C_{22} derivatives appear to exhibit the same position of this phase transition, while the gradual approach of the isotherms of the other three derivatives to $\pi = 0$ makes this determination very ambiguous, if not impossible.

The surface potential data shown in Figure 3 provide the first unambiguous evidence that only two longest chain derivatives (C_{20}- and C_{22}TEMPO) exhibit a critical point above room temperature. Using the Helmholtz equation

$$\mu_Z = (\Delta V)(\mathrm{MMA})\epsilon\epsilon_0 \qquad (1)$$

the surface potential (ΔV) measurements were interpreted in terms of the normal component of the effective molecular dipole moment (μ_Z) and plotted versus MMA.[9,19,20] In a seminal paper, Vogel and Möbius demonstrated that the terminal methyl group contributes +0.35 D to the effective dipole model in monolayers with ordered, perpendicularly oriented alkane chains such as stearic acid.[19] In our case, however, the large cross sectional area of the TEMPO headgroup relative to that of the chain (even at small MMA's) is likely to allow the terminal methyl group sufficient conformational flexibility to minimize the contribution of its dipole moment to the measured μ_Z. Thus, the magnitude of μ_Z in Figure 3 is likely associated only with the TEMPO headgroup.

Only in the case of the C_{20}- and C_{22}TEMPO monolayers does μ_Z not appreciably change when these monolayers are spread on the water surface. In other words, the surface potential continues to be dominated by the background value of the clean water surface (defined as 0 D) and indicates the LE−G coexistence of these TEMPO monolayers. The sharp increase of μ_Z during monolayer compression clearly indicates completion of the LE/G phase transition. The smaller value of the MMA of this transition, which is reproducible to ±10 Å^2/molecule, recorded for C_{20}TEMPO is not clear to us. The supercritical state of the three shorter chain TEMPO monolayers is clearly evidenced by the high values of μ_Z at all MMA's. While surface potential measurements are notoriously difficult to interpret quantitatively,[9,20] the conspicuous, nonlinear decrease of the effective molecular dipole moment observed for all five monolayers at MMA < 100 Å^2/molecule is consistent with the hypothesis of the gradual rotation of the piperidine headgroup upon compression from approximately horizontal to vertical.[21]

The supercritical nature of the C_{14}−C_{18}TEMPO monolayers may seem surprising when viewed in comparison with aliphatic alcohols, acids, esters, and nitriles mentioned in the Introduction. In those cases, only the amphiphiles with the chain length not exceeding C_{12} were shown to exhibit $T_c^{(l)}$ below room temperature. We note that the recent results of Casson and Bain actually place $T_c^{(l)}$ of dodecanol above room temperature.[12] While the van der Waals chain−chain interactions constitute the major component of monolayer cohesiveness, a uniform correlation of LE/G critical temperature with the chain length can be expected only within a group of structurally similar amphiphiles.[9] The conspicuously large cross sectional area of the headgroup (particularly in a region of low surface pressures) of the TEMPO group relative to that of the alkane chain results in a decrease in the van der Waals interactions between the alkane chains due to their stearic inability to align over their full length. In effect, the large ratio of the headgroup to chain cross sectional areas renders the effective alkane chain length of the TEMPO amphiphiles to be significantly shorter than their physical length.

Brewster Angle Microscopy. The capability of Brewster angle microscopy to image the morphology of Langmuir monolayers and to determine phase transitions is well established.[22−24] Naturally, observation of a texture featuring coexistence of the liquid and gaseous phases at a particular MMA constitutes a proof that a LE/G phase transition did occur. Three examples of such images obtained for C_{22}TEMPO are shown in Figure 4. However, in cases when BAM images of homogeneous texture are obtained, even in a range of zero surface pressures, the opposite conclusion cannot be made with certainty. In an attempt to remove this ambiguity, in the experiments reported below, we measured the reflected light intensity of the BAM laser beam integrated over the entire illuminated area (ca. 320 × 430 μm^2) of the water surface. These data are plotted in Figures 5, 6, and 7 as a function of the C_n-TEMPO surface concentrations. The data representing individual amphiphiles were collected by increasing their surface concentration over the reported range. The latter corresponds to MMA's of ca. 450−50 Å^2/molecule. Each data point represents the integrated light intensity ("the gray level") at a particular concentration averaged over 30−90 s. The bars reflect the full range of random light intensity fluctuations recorded during that time. Despite active vibrational isolation, these fluctuations are caused by the vibrations of the water surface induced by mechanical vibrations beyond our control. The integrated-light

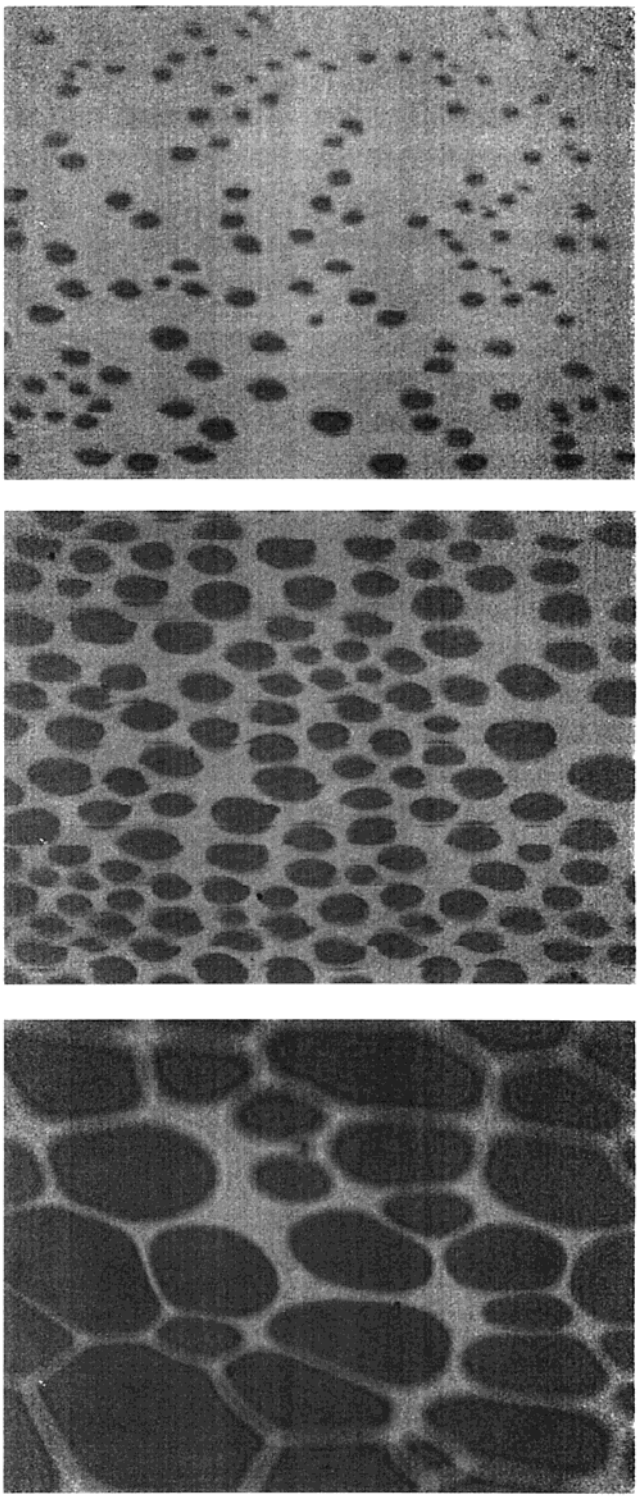

Figure 4. Brewster angle micrographs of C_{22}TEMPO monolayer recorded at (from top to bottom) 99, 105, and 130 Å^2/molecule with the other experimental conditions as those in Figure 2. The length of the horizontal edges of these images corresponds to 430 μm.

intensity at 5×10^{-11} mol cm^{-2} and at lower concentrations is the same as the value measured for the clean water surface.

Figure 5 presents the plots of the light intensity obtained for C_{14-18}TEMPO monolayers. The linearity of these plots reveals the linearly varying density of the TEMPO monolayers over the full range of their apparent surface concentrations from a high-pressure region to ca. 450 Å^2/molecule. On the basis of this evidence, we conclude that these three members of the TEMPO group do not undergo a phase transition. In other words,

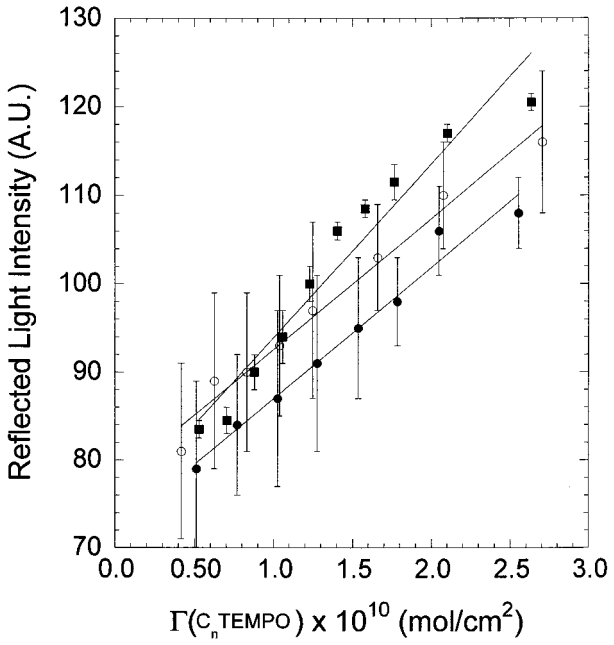

Figure 5. Plots of the average, reflected BAM light intensities integrated over the area of illumination of 320×430 μm^2 vs surface concentration of C_{14}TEMPO (closed circles), C_{16}TEMPO (open circles), and C_{18}TEMPO (closed squares). The error bars correspond to the full range of random light intensity fluctuations observed at each MMA over ca. 30−90 s exposures. The other conditions are given in Figure 2.

their LE/G critical temperatures appear to be below 23.5 °C. This conclusion is consistent with the surface potential measurements shown in Figure 3. Needless to say, exhaustive BAM monitoring of these three monolayers in the range of concentrations explored in Figure 5 have never yielded a biphasic texture that would be expected for a LE−G coexistence. We should point out that the somewhat nonlinear behavior of C_{18}TEMPO in these experiments is not clear to us. As discussed below, presence of a weak inflection point in the C_{18}TEMPO data set could suggest proximity of $T_c^{(l)}$ for this compound. However, linear plots of light intensity versus surface concentration which did not exhibit this small inflection were also obtained for C_{18}-TEMPO at 6 and 0 °C. The surface potential and 2D electrochemistry data (see below) also did not give any evidence of a phase transition for C_{18}TEMPO. Consequently, we include this amphiphile together with the other two in Figure 5 in the group of 2D supercritical fluids.

Figure 6 shows the results of the same type of experiments for the C_{20}- and C_{22}TEMPO monolayers. Clearly, the behavior of these two compounds at 23.5 °C is substantially different. At surface concentrations below ca. 1.7×10^{-10} mol/cm^2 (corresponding to MMA > 100 Å^2/molecule), a two-phase region of LE and G phases is always observed, with the area fraction covered by the 2D gas phase increasing as the monolayers are expanded (see also Figure 4). The fluctuations of the reflected light intensity in this region are due to a usual monolayer flow and correspond to the variable fractional surface area covered by each of the LE and G phases within the illuminated area of 320×430 μm^2. While only two data points are marked for each surface concentration in this region, we observed and recorded essentially all levels of reflected light intensities between the high and low values shown in Figure 6. These fluctuations gradually disappear when the apparent surface concentration of an amphiphile decreases below ca. 8×10^{-11} mol/cm^2. In that region, as the size of the gas domains and the

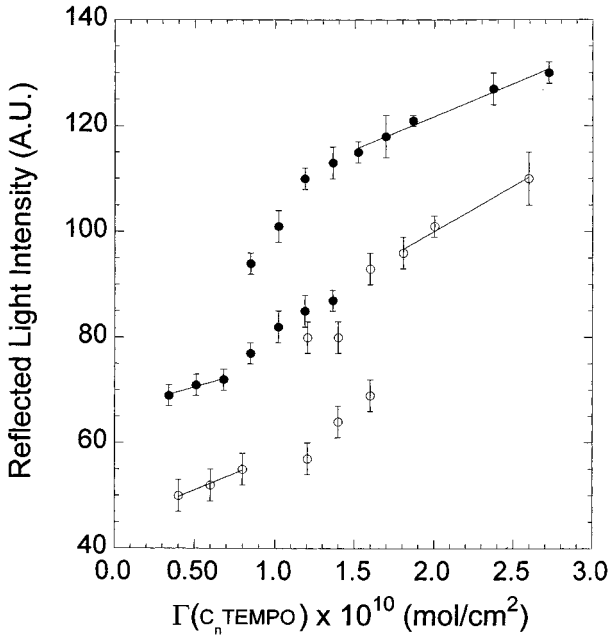

Figure 6. Plots of the average, reflected BAM light intensities integrated over the area of illumination of 320 × 430 μm^2 vs surface concentration of C_{20}TEMPO (open circles) and C_{22}TEMPO (closed circles). The pairs of the light intensities each shown for a given MMA correspond to the minimum and maximum values of the reflected light recorded at that MMA. These result from the fluctuations in the density and size of the G and LE domains observed in the illuminated area due to monolayer flow. The bars correspond to the full range of random light intensity fluctuations observed for each measurement over ca. 30−90 s exposures. The other conditions are given in Figure 2.

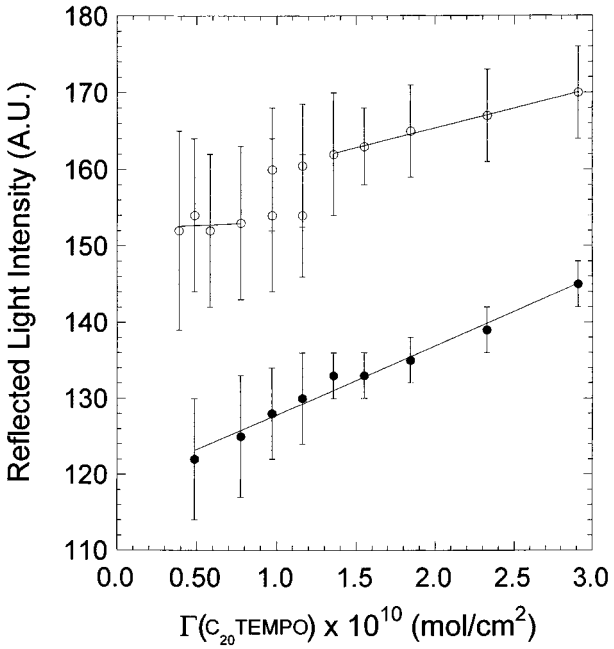

Figure 7. Plots of the average, reflected BAM light intensities integrated over the area of illumination of 320 × 430 μm^2 vs surface concentration of C_{20}TEMPO recorded at 27 °C (open circles) and 29 °C (closed circles). The pairs of the light intensities shown for the same MMA in the experiment done at 27 °C correspond to the minimum and maximum values observed in the LE−G coexistence region. The other details and conditions are given in Figure 6.

fraction of the surface area covered by the gas phase continue to increase, the probability of observing simultaneously LE and G coexisting within the small laser illuminated area decreases and becomes negligible. We note that since the compositions of the G and LE phases in the LE−G two-phase region are constant, the reflected light intensity is expected to be ultimately constant. The three data points at the lowest surface concentrations in Figure 6 lead to that region.

Experiments such as those of Figure 6 do not provide an accurate means of measuring the onset of the LE/G phase transition. This is due to the small size of the monolayer area probed by BAM. For example, if during monolayer compression the small "bubbles" of the 2D gas phase are no longer seen in the area probed by BAM but persist elsewhere and are thus unnoticed, the MMA corresponding to the end of the two-phase region may be overestimated. This difficulty notwithstanding, if the BAM monitoring is extended to a sufficiently long time (ca. 3 min; see Experimental Section) at each new MMA, the position of the phase transition can be measured reproducibly. In these types of experiments, we did not observe any histeresis for the C_{22}TEMPO system. In other words, the position of the phase transition did not depend on whether it was measured during slow, stepwise monolayer expansion or compression. Specifically, C_{22}TEMPO has a phase transition at 99 ± 1 Å^2/molecule. The precision of these measurements reflects largely the uncertainty in the determination of the surface area. Since these measurements involve times of several minutes, factors such as the small solubility of the amphiphiles are responsible for this uncertainty.

The position of the phase transition of C_{20}TEMPO, 127 ± 3 Å^2/molecule is more difficult to determine. The value given here was obtained in the compression experiments in which disappearance of the LE−G coexistence region is taken as the position of the LE/G phase transition. Unlike what we reported for the C_{22}TEMPO system, an attempt to determine the position of the LE/G phase transition during a gradual expansion of the C_{20}TEMPO LE phase is associated with a large histeresis of ca. 40−60 Å^2/molecule. Clearly, in this case, the kinetic barrier to nucleate the gas phase is substantial. The existence of such barriers and related phenomena are well-known and are related to a decreased equilibrium vapor pressure (P) of a substance in a cavity of small radius (r) relative to the equilibrium vapor pressure measured above a flat surface (P_0) (see eq 2).[25] Similarly, the Kelvin equation predicts the equilibrium vapor pressure to be higher for a droplet of liquid of small radius:

$$RT \ln\left(\frac{P}{P_0}\right) = \pm \frac{2\gamma V_m}{r} \qquad (2)$$

Here γ is the surface tension of the liquid/vapor interface, and V_m is the molar volume of the substance. The plus and minus signs apply to the cases of small droplets of liquid and small cavities of vapor, respectively, as encountered near G/L and L/G phase transitions. In the former case, the increased equilibrium vapor pressure of a small droplet of liquid results in a commonly observed supersaturation of the vapor phase.[25] The fact that the expansion of C_{20}TEMPO monolayer does not result in a LE/G phase transition at the same MMA as that associated with the collapse of the G−LE coexistence region during compression is a pronouncement of the instability of a vapor phase in small 2D cavities described by the 2D version of the Kelvin equation. What is surprising is the substantial discrepancy in the behavior of the two rather similar monolayer systems C_{20}TEMPO and C_{22}TEMPO. We believe that this is related to the low value of the C_{20}TEMPO critical temperature. Indeed, consideration of the higher-temperature BAM data in Figure 7 confirms this. While the plot of the reflected light intensity vs surface concentration obtained at 27.0 °C clearly

exhibits a coexistence region consistent with the LE/G phase transition at ca. 130 Å^2/molecule, the same experiment carried out at 29 °C yielded a linear dependence of the reflected light intensity on the surface concentration over its entire range. Needless to say, BAM images never revealed coexistence-type textures at this temperature. Thus, the critical temperature for C_{20}TEMPO can be estimated to be 28 °C. We note that phase nucleation near the critical temperature was treated theoretically by McGraw and Reiss.[26] Their prediction of an increased barrier for nucleation under such conditions is reflected, albeit in 2D, in the data presented above. We further note that preliminary measurements of the reflected light intensities vs surface concentration done for C_{18}TEMPO yielded linear plots at temperatures as low as 0 °C. Thus, the difference between C_{20}- and C_{18}TEMPO $T_c^{(l)}$ values is greater than 28 °C, suggesting that this homologous series of surfactants does not reflect a commonly accepted rule of "equivalent states" which states that a one carbon addition to the alkane chain changes monolayer properties of an amphiphile in nearly the same fashion as a 5−10 °C decrease of temperature.[9,27]

2D Electrochemistry. In our previous paper, we reported a discontinuity in the 2D voltammetry of tetradecane ferrocene-ketone (C_{14}Fc) upon slow expansion of its monolayer on the water surface.[14] Our observations indicated that the 2D voltammetric "line" microelectrode which resides by self-positioning exactly in the plane of the air/water interface functions as a nucleating site for the monolayer gas phase. Once nucleated at the line microelectrode, the gas phase isolates this sensor from the LE phase, and the current signal abruptly vanishes, as the surface concentration of the amphiphile in the G phase is substantially lower and below detection limit of 2D voltammetry. We were able to reproducibly determine (within ±2 Å^2/molecule) the position of the LE/G phase transition by 2D voltammetry both during C_{14}Fc monolayer expansion and compression.[14] In the latter case, the appearance of the current signal coincided with the final collapse of the coexistence region.

We now consider similar experiments done with the C_{14-22}TEMPO monolayers. As reported previously for C_{14}-TEMPO, the three monolayers with the shorter chains, those with $T_c^{(l)}$ below room temperature, did not show any discontinuities in 2D voltammetric experiments even following prolonged equilibration of their monolayers at 450 Å^2/molecule. In the case of the two longer chain derivatives, C_{20-22}TEMPO, 2D electrochemistry can be used to determine the position of their LE/G phase transition. Two types of experiments can be done to accomplish this. Both are illustrated in Figure 8 using C_{22}TEMPO. The first experiment is analogous to that described above for the C_{14}Fc case. A line microelectrode is positioned at the water surface in the LE region of the monolayer and a 2D voltammogram is recorded. The monolayer is then expanded in small steps and current voltage curves are recorded after each expansion. Initially (see Figure 8A, curve 1), a well-developed Faradaic current is observed as expected for the LE state. Once the MMA of the phase transition is reached, the current begins to oscillate (curve 2) and then decays to a background level (curve 3). The oscillations can be associated with the presence of small 2D cavities of the gas phase newly generated at the line microelectrode. Since compressibility of the gas phase is naturally larger than that of the LE phase, small mechanical vibrations in the monolayer result in the observed fluctuations in the length of the microelectrode remaining in contact with the LE phase. The observed frequency of these fluctuations of 7−10 Hz, which corresponds to the frequency of the mechanical laboratory noise, and the increase of their amplitude when vibration isolation is turned off are consistent with this explanation. The oscillations and the average magnitude of the Faradaic current at this MMA decrease slowly to zero with time and upon further expansion of the monolayer. This behavior is reversible upon recompression of the monolayer as shown in Figure 8A, curve 4.

The same experiment can be initiated in a LE−G coexistence region. Initially, only the capacitive background is recorded (see Figure 8B, curves 1 and 2). When the monolayer compression reaches the point of the phase transition (the end of the coexistence region), the oscillatory behavior of the Faradaic current is observed as shown in Figure 8B, curve 3. Further compression yields a fully developed 2D voltammogram. In these types of experiments, the position of the phase transition can be accurately measured if the MMA of the initial positioning of a fresh electrode is close to the phase transition and if the expansion or compression is carried out in small steps. The experiments of Figure 8A,B were done under such conditions and yielded the correct (see below) position of the phase transition of 98 Å^2/molecule. However, if these conditions are not met, the 2D electrochemical results can lead to an erroneous conclusion. For example, consider the experiment in Figure 8C. After recording the first voltammogram at 97 Å^2/molecule which indicated correctly the LE state of the monolayer, the monolayer was expanded to 105 Å^2/molecule. At this point, the monolayer is certainly in the coexistence region. Yet voltammogram 2 in Figure 8C exhibits the same oscillatory behavior as what we associated above with the onset of the phase transition. Clearly, such interpretation of this result would result in an error.

The performance of the line microelectrodes described in Figure 8C is revealing in that it implies an affinity of the microelectrode for the LE phase that could lead to a delayed (erroneous) reporting of the LE/G phase transition. Additional investigations of this and related phenomena showed that fresh line microelectrodes (those never exposed to the air/water interface) exhibit a remarkable and unmistakable ability to differentiate between the LE and LE−G states of the monolayer. Consider the following experiment. After an approximate position of the phase transition is determined using 2D voltammetry during monolayer expansion or compression experiments as described above, the definitive test involves simply placing a fresh line microelectrode at a monolayer covered interface at a specific MMA and recording a 2D voltammogram. This is illustrated in Figure 8D. In the case of C_{22}TEMPO monolayers at 99 Å^2/molecule or higher, the response of a fresh electrode is always limited to a capacitive background, indicating that the electrode is in contact exclusively with the G phase. At 98 Å^2/molecule (or smaller), the same experiment with a fresh microelectrode invariably yields a well developed Faradaic signal, indicating that the electrode is in contact exclusively with the LE phase of the monolayer. This behavior was observed consistently with over 100 microelectrodes examining the state of the C_{22}TEMPO monolayers (in several independently spread monolayers) around the LE/G phase transition. We observed no exceptions from this behavior of fresh line microelectrodes. This remarkable consistency in the behavior of fresh line microelectrodes allows us to conclude that at 23.5 °C the LE/G phase transition must occur at 98.5 ± 0.5 Å^2/molecule.

The consistent ability of fresh microelectrodes to unambiguously determine the state of the monolayer within just 1 Å^2/molecule around the point of the LE/G phase transition is even more remarkable when one compares the size of a line electrode (500 μm in length) with the average size and density of the 2D gas cavities. The latter two can be assessed from the BAM

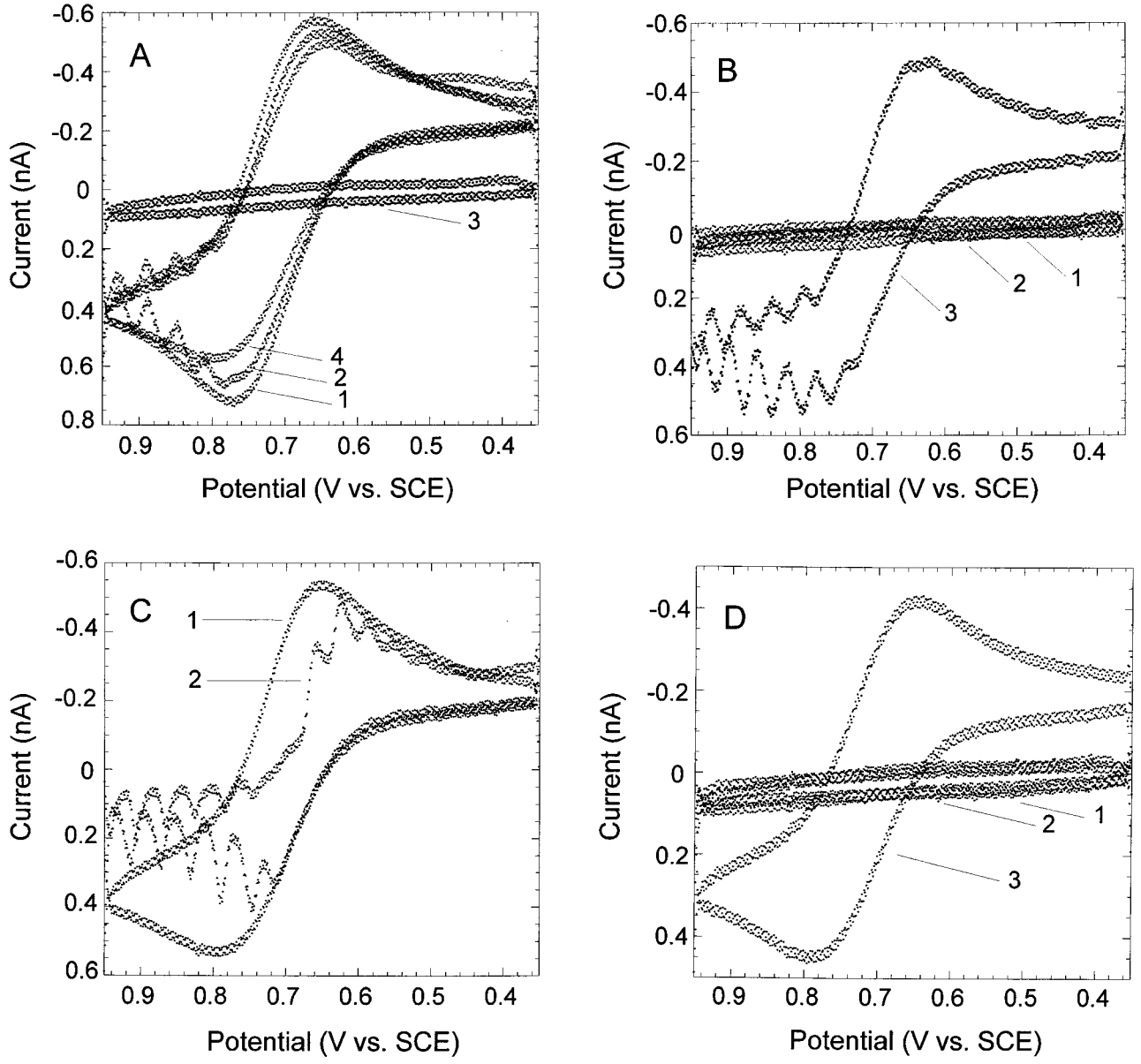

Figure 8. 2D voltammetry of C_{22}TEMPO at the air/water interface (50 mM HNO_3 subphase). All curves in each of the panels A−C were recorded at the same line electrode. In panel D, each 2D voltammogram was recorded at a fresh line microelectrode. The 2D voltammograms were recorded at the following MMA's: A, curves 1−4 correspond to 97, 99, 101, and 98 Å^2/molecule, respectively; B, curves 1−3 correspond to 102, 100, and 98 Å^2/molecule, respectively; C, curves 1 and 2 correspond to 97 and 105 Å^2/molecule, respectively.; D, curves 1−3 correspond to 100, 99, and 98 Å^2/molecule, respectively.

images of the monolayer at 99 Å^2/molecule such as that shown in Figure 4. Examination of these images yields the average diameter of a gas cavity of 5−20 μm. While their density fluctuates from one region of the monolayer to the next, it is relatively low. Since the consistent absence of the Faradaic signal under these conditions (Figure 8D, curves 1 and 2) must be associated with the fact that the entire 500 μm length of a line electrode is in contact with the 2D gas phase, it is clear that the line electrodes function as nucleating sites of the G phase.

Similarly to the diminished capabilities of BAM to detect LE/G phase transition in C_{20}TEMPO monolayers, the ability of the line microelectrodes to accomplish this is also less effective. Just as in the BAM experiments, nucleation of the G phase at a microelectrode during stepwise expansion of these monolayers is burdened with a large histeresis of as much as 30 Å^2/molecule. When a C_{20}TEMPO monolayer in the LE−G coexistence region is slowly compressed, the appearance of the well developed 2D signal was first observed in the range of 130 to 125 Å^2/molecule. This is consistent with the BAM result reported above. The behavior of fresh line microelectrodes to detect the 2D G phase is also less precise. The point nearest to the phase transition at which LE phase was detected was not as sharply defined as in the C_{22}TEMPO case and involved a range of MMA's of 127−130 Å^2/molecule. Naturally, the proximity of the critical temperature to the room temperature of this monolayer and the expected diminished differences between the physical properties of the LE and G phases of C_{20}TEMPO are responsible for these results. An interesting pronouncement of the diminished differences between LE and G phases is an increased equilibrium concentration of the C_{20}TEMPO in the gas phase. While the surface concentration of the C_{22} derivative in the G phase is clearly below the detection limits of the 2D voltammetry, the higher G phase concentration of the C_{20} derivative allows us to record a measurable Faradaic current in this phase. Its magnitude gives an estimate of the C_{20}TEMPO

gas-phase concentration of $1.1 \pm 0.4 \times 10^{-11}$ mol/cm^2 (corresponding to a MMA of 1500 Å^2/molecule). Characterization of the properties of the LE and G phases near the critical temperature is a subject of current investigations.

Conclusions

We focused on the comparison of BAM and 2D electrochemistry as two independent techniques capable of determining the position of the LE/G phase transition and the value of the 2D critical temperature of C_{20-22}TEMPO monolayers. We showed that by constructing plots of the integrated intensity of the reflected BAM laser light versus the amphiphile's surface concentration for several values of temperature, one observes linear plots above the critical point, and that below the critical temperature, such plots exhibit a distinct inflection with multiple values of the reflected light intensities at each surface concentration below the LE/G phase transition. Using this approach, we determined the C_{20}TEMPO LE/G critical temperature to be 28 °C.

BAM and 2D voltammetry can also be used to determine the position of the LE/G phase transition. Using C_{22}TEMPO monolayers as a test case, we found that both techniques are equally accurate and precise. BAM requires a somewhat time-consuming set of measurements in the immediate vicinity of the phase transition. Since in this technique only the images featuring a LE−G coexistence texture can be unambiguously interpreted, one must minimize a possibility of "false negative" type results. Contrary to this feature of BAM, the very nature of the phenomena allowing 2D voltammetry to determine the phase transition circumvents such uncertainties offering unambiguous results at MMA's both below and above the phase transition. We find this feature of the 2D voltammetric method to be clearly superior relative to BAM. To expand on this point: we discovered that fresh line microelectrodes exhibit a remarkably consistent ability to nucleate the 2D gas phase and become fully contacted by the gas phase. Consequently, whenever a fresh microelectrode is placed at the air/water interface covered with a C_{22}TEMPO monolayer in a LE−G coexistence region, the 2D gas phase is immediately nucleated along its entire length. This then yields only a small capacitive current signal in this region. A 2D voltammetric signal featuring a large Faradaic current is always observed if a fresh electrode is placed in contact with a monolayer in the LE state. Thus, within a 1 Å^2/molecule change in MMA around the phase transition, the 2D current switches between the on/off levels with a ratio of ∼50. This consistent ability of line electrodes to nucleate the 2D gas phase (also observed in the case of C_{14}Fc monolayers[14]) is perhaps related to the hydrophilic character of clean gold, which is newly generated when a line electrode is created by fracturing a gold-coated glass slide (see Experimental Section). Thus, at the first contact with the monolayer on the water surface, the clean surface of the gold edge is hydrated and, following nucleation of the 2D gas phase, prefers to stay in contact with that phase rather than to contact a more lipophilic LE phase of the monolayer. We note, however, that the line electrodes, once exposed to the LE phase, no longer exhibit the affinity for the G phase that the fresh electrodes do. This leads, in experiments such as that in Figure 8C, to a delayed nucleation of the 2D gas phase upon monolayer expansion. Interestingly enough, microelectrodes first exposed to the 2D gas phase also exhibit a somewhat delayed response when monolayer compression results in elimination of the LE−G coexistence region. To reiterate the main observation: only fresh line microelectrodes can consistently show the high/low type current signal when first contacting the LE or LE−G states of the monolayer, respectively.

Acknowledgment. We are grateful to Professor Rebecca Braslau for suggesting significant modifications to the procedure of the C_nTEMPO synthesis and for her hospitality at UC Santa Cruz, where the modified synthesis was first carried out. This research was supported financially by the U.S. National Science Foundation under Grant CHE-0079225.

References and Notes

(1) Kaganer, V. M.; Möhwald, H.; Datta, P. *Rev. Mod. Phys.* **1999**, *71*, 779−819.
(2) Knobler, C. M. *Science* **1990**, *249*, 870−874.
(3) Knobler, C. M.; Rashmi, C. D. *Annu. Rev. Phys. Chem.* **1992**, *43*, 207−236.
(4) McConnell, H. M. *Annu. Rev. Phys. Chem.* **1991**, *42*, 171−195.
(5) Henon, S.; Meunier, J. *Rev. Sci. Instrum.* **1991**, *62*, 936−939.
(6) Hönig, D.; Mobius, D. *J. Phys. Chem.* **1991**, *95*, 4590−4592.
(7) Als-Nielsen, J.; Jackuemain, D.; Kjaer, K.; Leveiller, F.; Lavav, M.; Leizerowitz, L. *Phys. Rep.* **1994**, *246*, 251−313.
(8) Adam, N. K.; Jessop, *G. Proc. R. Soc. London, Ser. A* **1926**, *110*, 423−441.
(9) Gaines, G. L. J. *Insoluble Monolayers at Liquid-Gas Interfaces*; Wiley-Interscience: New York, 1966.
(10) Knobler, C. M. Recent Developments in the Study of Monolayers at the Air-water Interface. In *Advances in Chemical Physics*; Progogine, I., Rice, S., Eds.; Wiley: New York, 1990; Vol. 77, pp 397−449.
(11) Moore, B. G.; Knobler, C. M.; Akamatsu, S.; Rondelez, F. A. *J. Phys. Chem.* **1990**, *94*, 4588−4595.
(12) Casson, B. D.; Bain, C. D. *J. Am. Chem. Soc.* **1999**, *121*, 2615−2616.
(13) Pfohl, T.; Möhwald, H.; Riegler, H. *Langmuir* **1998**, *14*, 5285−5291.
(14) Johnson, M. J.; Anvar, D. J.; Skolimowski, J. J.; Majda, M. *J. Phys. Chem. B* **2001**, *105*, 514−519.
(15) Majda, M. Translational Diffusion and Electron Hopping in Monolayers at the Air/Water Interface. In *Organic Thin Films nad Surfaces*; Ulman, A., Ed.; Academic Press: San Diego, 1995; Vol. 20, pp 331−347.
(16) Charych, D. H.; Landau, E. M.; Majda, M. *J. Am. Chem. Soc.* **1991**, *113*, 3340−3346.
(17) Wittek, M.; Möller, G.; Johnson, J. J.; Majda, M. *Anal. Chem.* **2001**, *73*, 870−8777.
(18) Johnson, M. J. Ph.D. Dissertation, UC Berkeley, Berkeley, CA, 2001.
(19) Vogel, V.; Möbius, D. *J. Colloid Interface Sci.* **1988**, *126*, 408−420.
(20) Taylor, D. M. *Adv. Colloid Interface Sci.* **2000**, *87*, 183−203.
(21) The dependence of the effective dipole moment of the TEMPO amide headgroup on its orientation with respect to the water surface was investigated numerically using the QChem density functional package. In general, these calculations support our hypothesis. However, since several assumptions have to be made concerning plausible conformations of the two polar groups of this amphiphile and the headgroup orientation with respect to the water surface, we cannot credibly offer these results as a quantitative proof of this hypothesis.
(22) Overbeck, G. A.; Möbius, D. *J. Phys. Chem.* **1993**, *97*, 7999−8004.
(23) Rivier, S.; Henon, S.; Meunier, J.; Schwartz, D. K.; Tsao, M.-W.; Knobler, C. M. *J. Chem. Phys.* **1994**, *101*, 10045−10051.
(24) Melzer, V.; Vollhardt, D.; Brezesinski, G.; Möhwald, H. *J. Phys. Chem. B* **1998**, *102*, 591−597.
(25) Adamson, A. W.; Gast, A. P. *Physical Chemistry of Surfaces*, 6th ed.; Wiley: New York, 1997.
(26) McGraw, R.; Reiss, H. *J. Stat. Phys.* **1979**, *20*, 385−413.
(27) Peterson, I. R.; Brzezinski, V.; Kenn, R. M.; Steitz, R. *Langmuir* **1992**, *8*, 2995−3002.